ISSN 0036-0295, Russian Metallurgy (Metally), Vol. 2018, No. 9, pp. 808–814. © Pleiades Publishing, Ltd., 2018.
Original Russian Text © M.Yu. Kollerov, D.E. Gusev, S.I. Gurtovoi, A.V. Burnaev, 2018, published in Metally, 2018, No. 5, pp. 17–25.

# Thermomechanical Behavior of Titanium Nickelide-Based Alloys at a Constant Counteraction

**M. Yu. Kollerov[a], *, D. E. Gusev[a], S. I. Gurtovoi[a], and A. V. Burnaev[a]**

[a] *Moscow Aviation Institute (National Research University), Moscow, Russia*

**e-mail: mitom@implants.ru*

Received July 12, 2017

**Abstract**—The influence of a constant counteraction on the shape recovery and the specific shape recovery energy in a titanium nickelide-based alloy is considered. This energy is shown to be maximal after preliminary deformation of the material to a critical value and the external counteraction of shape recovery that corresponds to critical stresses. The specific shape recovery energy is maximal in a titanium nickelide-based alloy with the structure recrystallized at an annealing temperature of 570°C.

*Keywords*: titanium nickelide, shape memory effect, superelasticity, heat treatment, structure, properties, work, counteraction

**DOI:** 10.1134/S0036029518090082

## INTRODUCTION

Titanium nickelide–based alloys with the shape memory effect (SME) and superelasticity are most used to produce thermomechanical joints, thermoforce actuators, and medical implants, which undergo counteraction from other structural members or the environment [1–5]. The elements made of titanium nickelide tend to recover their initial shape and do the corresponding work, which is determined by the chemical composition and the structure of an alloy and deformation and heating conditions. Information on this work is necessary to design most SME materials. Moreover, counteracting loads change the temperature (temperatures of the onset and end of shape recovery $A_s^r$ and $A_f^r$, respectively) and deformation (strains $\varepsilon_r$ and $\gamma_r$ to be recovered) characteristics of titanium nickelide articles, which hinders the prediction of the behavior of these articles during operation [6].

The conditions of shape recovery counteraction can be schematically divided into the following two types [7]: at a gradually increasing load and at a constant counteracting load. In the first case, the reactive stresses in a material increase in heating when its shape is recovered [8–10]. These stresses depend substantially on the stiffness of a counteracting device: for example, when couplings are restored for assembling thermomechanical joints, the pipes to be joined prevent the coupling from reaching its initial size [7]. In the second case, counteraction causes constant temperature-independent stresses, which are operative during the entire shape recovery, in a material. This situation is illustrated by the devices that lift loads using SME elements. The purpose of this work is to consider this type of counteraction.

## EXPERIMENTAL

We studied the wire fabricated by drawing rods made of a TN1 titanium nickelide alloy containing 54.5% Ni (titanium for balance).[1] Alloy ingots were prepared by melting of iodide titanium and electrolytic nickel in a vacuum arc furnace with a nonconsumable tungsten electrode in a purified helium atmosphere on a water-cooled bottom (six melting processes). The impurity contents in the alloy were as follows: 0.07 O, 0.02 N, 0.006 C, and 0.002 H. The presence of an oxygen impurity in the alloy promotes the formation of the $Ti_4Ni_2O$ phase, which results in nickel enrichment of the *B*2 matrix. The results of metallographic studies demonstrate that the volume fraction of this phase is at least 10%. Using differential scanning calorimetry, we found that annealing of the alloy at 450–900°C for 1 h did not change the martensite transformation temperature ($M_s = -10 \pm 5$°C, $A_s = 20 \pm 3$°C), which indicate the absence of precipitation or dissolution of nickel-rich intermetallic particles ($Ti_3Ni_4$, $Ti_2Ni_3$).

Drawing was carried out at 600–700°C to reach w wire diameter of 1.5 mm, cold drawing was then performed to a final wire diameter of 1.3 mm, and the total deformation was 15–20%. Heat treatment of wire samples was conducted at 450 and 570°C in furnaces with an air atmosphere and at 900°C in vacuum. The microstructure of the samples was studied on a Neo-

[1] Hereafter, the element contents are given in wt %.

phot 31 optical microscope after electrochemical polishing and chemical etching.

The heat-treated samples were subjected to testing on a universal UPK 1 torsion device, which was based on the design of an inverse torsion pendulum, in a tube furnace with an air atmosphere in the temperature range 20–200°C (Fig. 1). The samples were deformed by torsion to various levels of tangential stresses $\tau$, shear strain $\gamma$ was measured, and $\tau$–$\gamma$ deformation diagrams were plotted using testing results. To determine the shape recovery energy, the samples were deformed by torsion at a temperature of 20°C and then heated in a loaded state under the action of the constant tangential stress specified by the load suspended from a torsion pendulum. The change in the angle of sample rotation with temperature was fixed upon heating. During shape recovery, the sample "untwisted" and lifted the load. The shape recovery energy was determined as the product of the mass and the displacement of the load. Using the ratio of this product to the sample volume, we calculated the specific shape recovery energy ($a_r$).

To determine the temperatures of the onset ($A_s^r$) and the end ($A_f^r$) of shape recovery, the samples were deformed by torsion by 3% at 20°C and then heated in the free-standing state to record the recovered strain as a function of the temperature gradient temperature. With these curves, we determined temperatures $A_s^r$ and $A_f^r$ similarly to the technique described in [11].

It should be noted that there are no generally accepted and standardized SME and superelasticity characteristics and methods for their determination. Therefore, we hope that the data obtained in this work will facilitate progress in this field, development of certain normative documents, and a wide discussion.

## RESULTS AND DISCUSSION

The structure and the thermomechanical behavior of the wire samples in the initial state (after drawing and polishing) are caused by intense cold working of the material in drawing a wire at temperatures below the recrystallization temperature of the alloy [12]. Therefore, we annealed the samples at 450, 570, and 900°C for 1 h under an external counteraction to study the influence of the structure of the alloy on its ability to recover shape under an external action. At 450°C, polygonization occurs in deformed semiproducts made of titanium nickelide–based alloys [13]. Recrystallization of this material begins above 550°C, and normal grain growth takes place with intense *B*2-phase grain growth upon heating above 800°C (Fig. 2). Therefore, heat treatment ensured the formation of different structural states of the material, which exhibited SME during deformation and heating. The temperature range of the onset and end of shape recovery in the heta-treated samples is given in Table 1.

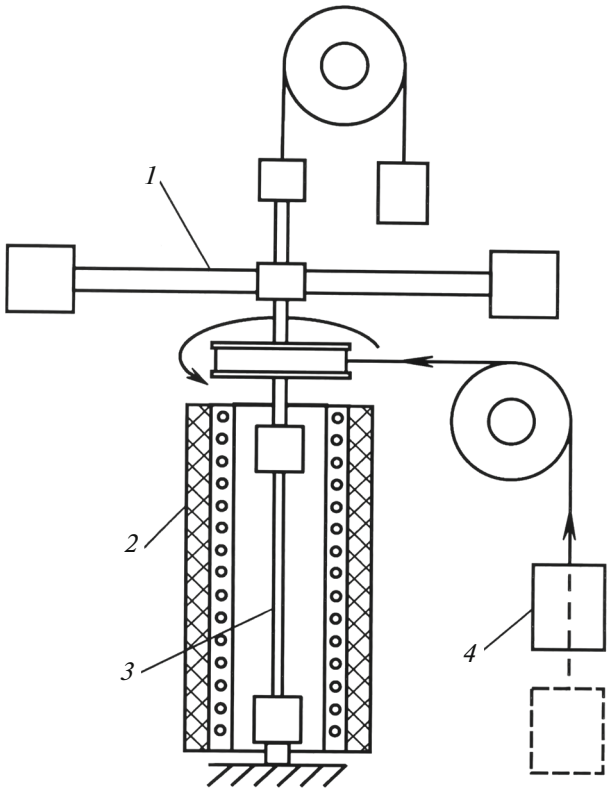


**Fig. 1.** Schematic diagram for testing a sample in an inverse torsion pendulum to determine the specific shape recovery energy: (*1*) inverse torsion pendulum, (*2*) furnace, (*3*) sample, and (*4*) load.

The structural state of the alloy substantially affects its mechanical behavior at normal temperature (Fig. 3). As compared to the annealed samples, the samples in the initial state are characterized by a relatively high yield strength, which is caused by the development of martensitic transformation under stress, and a high strain, which is elastically and/or superelastically recovered in unloading. The superelastic mechanism of strain recovery in unloading is indicated by a well-pronounced nonlinear character of the unloading curves. The residual strain fixed under these conditions is not fully recovered in the samples with the initial structure upon further heating. The yield strength of the annealed samples decreases significantly, the major part of the induced strain changes into residual strain after unloading, and this strain is fully or partly recovered upon further heating in the temperature range 30–60°C.

Intense slip develops in the alloy later as compared to the martensitic transformation under stress and induces mechanically and thermally irreducible strain. The maximum induced strain after which the initial sample shape is fully recovered upon unloading and/or further heating is called critical strain $\gamma_{cr}$ [14]. As the induced strain increases, the slip-induced unrecovered strain increases. To measure the critical

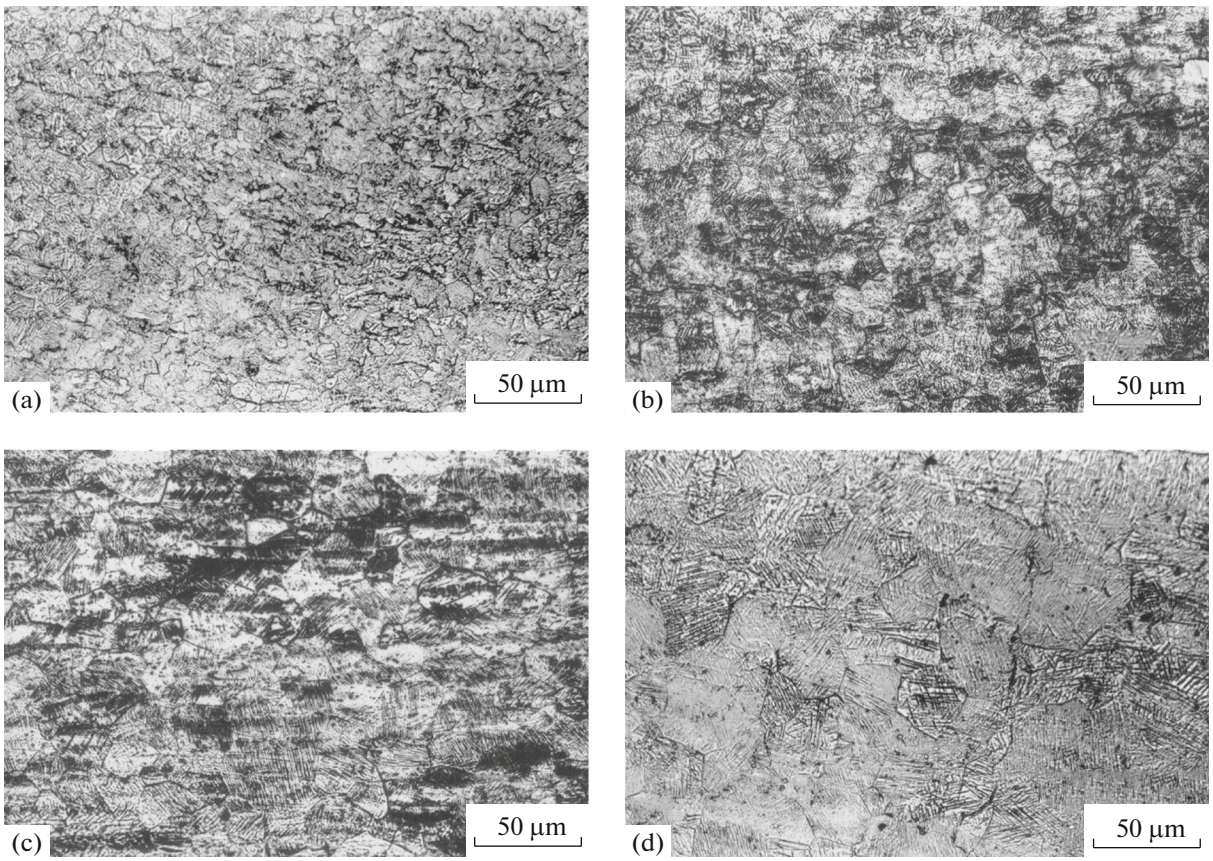


**Fig. 2.** Microstructure of a TN1 alloy in (a) initial state and after (b–d) annealing for 1 h at 450, 570, and 900°C, respectively.

strain, it is convenient to use the induced strain, which corresponds to the appearance of a certain small unrecovered strain specified by a strain tolerance (which is, e.g., 0.3% for torsion). This critical strain is designated as $\gamma_{cr}^{0.3}$ (Table 1, Fig. 4).

The experimental results demonstrate that the critical strain of the heat-treated samples is higher than that in the samples in the initial state (Table 1). This difference is caused by the fact that an increase in the annealing temperature leads to a decrease in the imperfection of the structure of the *B*2 matrix, which facilitates the stress-induced martensitic transformation and decreases the martensitic shear stress (see Fig. 3). However, a decrease in the structural imperfection promotes slip processes. Therefore, critical stress $\tau_{cr}^{0.3}$, which is determined from the $\tau$–$\gamma$ curves of the samples at the induced strain corresponding to $\gamma_{cr}^{0.3}$, also decreases upon annealing (see Table 1).

**Table 1.** Thermomechanical properties of wire samples made of atomic transition-based alloy

| Treatment conditions (state of sample) | $A_s^r$ | $A_e^r$ | $\gamma_{cr}^{0.3}$, % | $\tau_{cr}^{0.3}$, MPa | $a_r^{max}$, MJ/m$^3$ | | $G$, GPa (at 20°C) |
|---|---|---|---|---|---|---|---|
| | °C | | | | calculated | experimental | |
| Untreated (initial deformed) | 30 | 46 | 4 | 230 | 1.0 | – | 7.3 |
| Annealing at 450°C, 1 h (polygonized) | 33 | 47 | 7 | 200 | 3.7 | 3.6 | 6.0 |
| Annealing at 570°C, 1 h (recrystallized) | 36 | 50 | 9 | 150 | 4.5 | 5.0 | 5.0 |
| Annealing at 900°C, 1 h (recrystallized) | 39 | 60 | 7 | 120 | 3.4 | 3.8 | 8.9 |

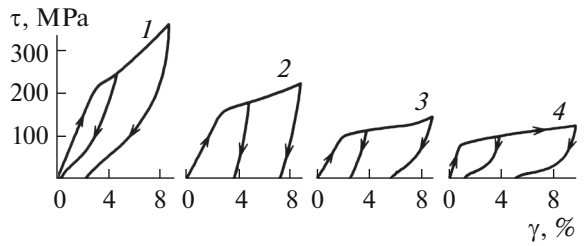


**Fig. 3.** Torsion curves at 20°C for TN1 alloy samples in (*1*) initial state and after annealing at 1 h for (*2*) 450, (*3*) 570, and (*4*) 900°C.

However, the decrease in the martensitic shear stress upon annealing turns out to be stronger than the decrease in the stresses inducing slip. As a result, an increase in the annealing temperature leads to an increase in $\gamma_{cr}^{0.3}$.

To determine the influence of the stresses acting against shape recovery on forming, we deformed samples at various degrees and normal temperature, loaded them to various levels of tangential stresses $\tau$ counteracting shape recovery, heated them to 140–160°C, and recorded the current value of strain $\gamma$. The difference between the strains in a sample after loading by counteracting stresses and the end of heating determined the strain recovered under load. After heating, the samples were cooled in a loaded state to normal temperature. The experimental results are shown in Figs. 5 and 6.

We now consider the thermomechanical behavior of the samples annealed at 570°C and deformed by 10% (see Fig. 5). After deformation by 10% and subsequent unloading, the samples retain a residual strain of ~7.2% at 20°C. This strain becomes higher after the application of a counteracting stress to be overcome by a sample to recover its initial shape upon subsequent heating. The sample shape is partly recovered upon heating in the temperature range from 40 to 140°C. The higher the counteracting stress $\tau$, the lower the recovered strain $\gamma_r$ and the higher the shape recovery temperature.

If the loaded samples are cooled to normal temperature, no forming is observed up-on cooling under the load lower than 80–100 MPa. At higher values of $\tau$, cooling causes deformation accumulation induced by the transformation plasticity when martensite forms under load. The strain having accumulated upon cooling increases with $\tau$ and exceeds an initial induced strain of 10% at the stresses higher than $\tau_{cr}^{0.3} = 150$ MPa.

Similar dependences of forming under load were observed when the preliminarily induced strain was lower (e.g., 6%) than the critical strain (see Fig. 6). In this case, the counteraction stress was limited to 80 MPa, since the deformation of the samples at normal temperature exceeds the given value (6%) at a higher stress.

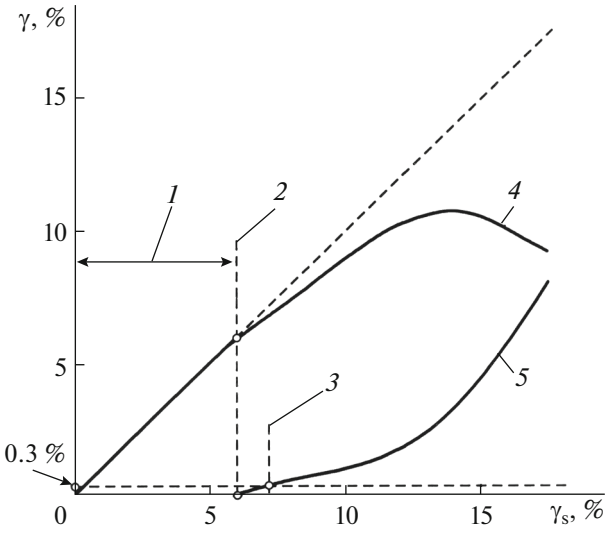


**Fig. 4.** Determination of the critical strain $\gamma_{cr}^{0.3}$ corresponding to the appearance of unrecovered strain (0.3%): (*1*) induced strain $\gamma_s$ is fully recovered, (*2*) critical strain $\gamma_{cr}$ above which unrecovered strain appears, (*3*) critical strain $\gamma_{cr}^{0.3}$ with a tolerance for an unrecovered strain of 0.3%, (*4*) sum of the elastic (superelastic) strain recovered upon unloading and the strain recovered upon heating ($\gamma_e + \gamma_r$), and (*5*) unrecovered strain $\gamma_{un}$.

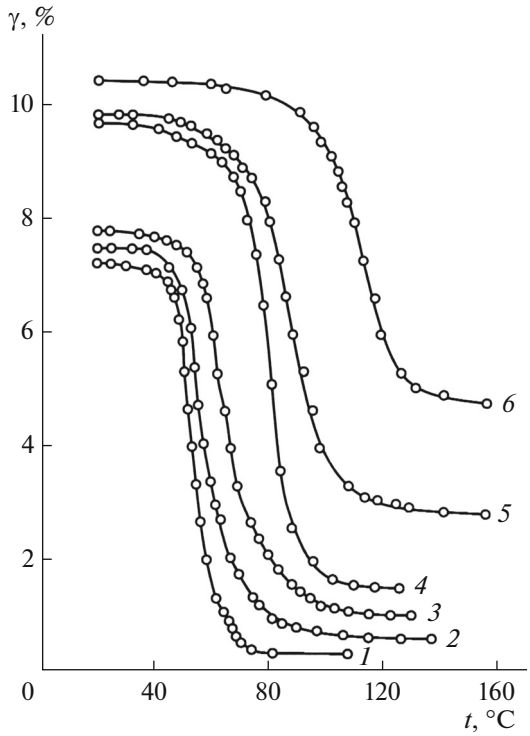


**Fig. 5.** Change in the shape of the TN1 alloy samples annealed at 570°C after deformation by 10% at 20°C in the course of heating at the counteraction stress (MPa): (*1*) without load, (*2*) 20, (*3*) 60, (*4*) 120, (*5*) 140, and (*6*) 180.

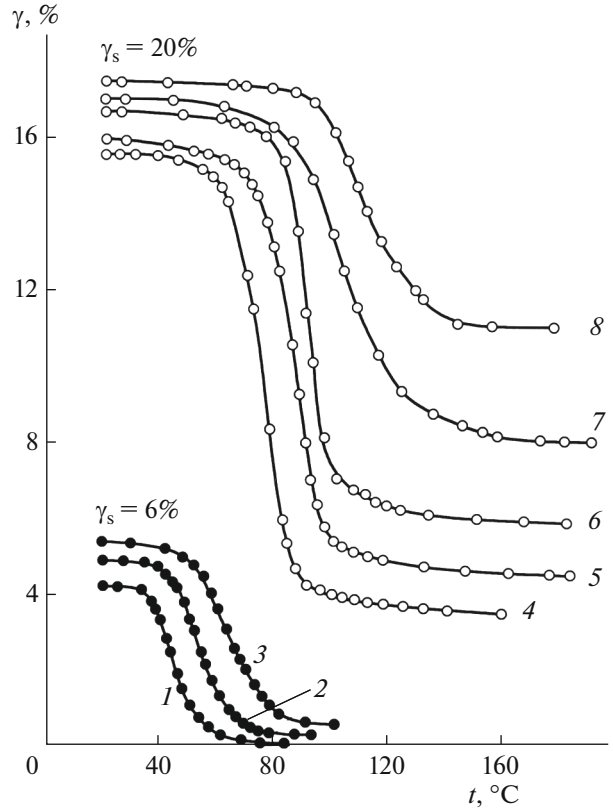


**Fig. 6.** Change in the shape of the TN1 alloy samples annealed at 570°C after deformation by (solid circles) 6 and (open circles) 20% at 20°C in the course of heating at the counteraction stress (MPa): (*1*, *4*) without load, (*2*, *5*) 40, (*3*, *6*) 80, (*7*) 100, and (*8*) 120.

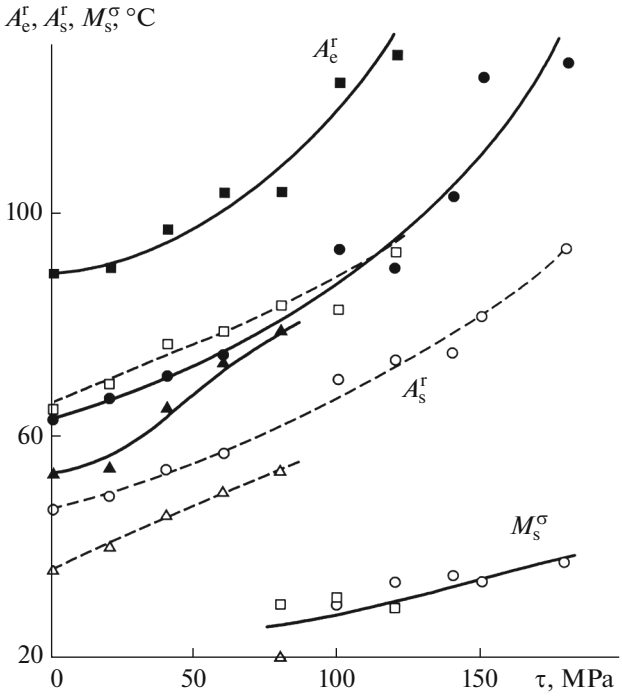


**Fig. 7.** Effect of counteraction stresses τ on the temperatures of the onset ($A_s^r$; open circles, dashed line) and end ($A_e^r$, solid circles, solid line) of shape recovery and the temperatures of the onset of martensitic transformation under load ($M_s^\sigma$, open circles, solid line). The preliminary strain is (△, ▲) 6, (○, ●) 10, and (□, ■) 20%.

At all induced strains (6, 10, 20%), the transformation plasticity upon cooling takes place at a stress higher than 80–100 MPa. The temperature of martensitic transformation under stress ($M_s^\sigma$) increases with the induced strain and counteraction stress (Fig. 7). The shape recovery temperatures ($A_s^r$, $A_e^r$) change similarly.

The calculations of the specific shape recovery energy show that it increases with the counteraction stress until the limiting value (Fig. 8). The dependence of $a_r$ on counteraction stress τ is influenced by preliminarily induced strain $\gamma_s$. When $\gamma_s$ is lower than the critical value, $a_r$ increases up to the values of τ corresponding to this strain at normal temperature. At strain $\gamma_s$ that is equal or close to $\gamma_{cr}^{0.3}$, the dependence of $a_s$ on τ is divided into the flowing two segments: in the first segment, this dependence increases monotonically, as in the previous case; in the second segment, this dependence is almost horizontal. The specific shape recovery energy is maximal at the counteraction stresses that are close to the stresses that cause slip in the alloy matrix. In this case ($\gamma_s > \gamma_{cr}^{0.3}$), the $a_r$–τ dependence has a maximum.

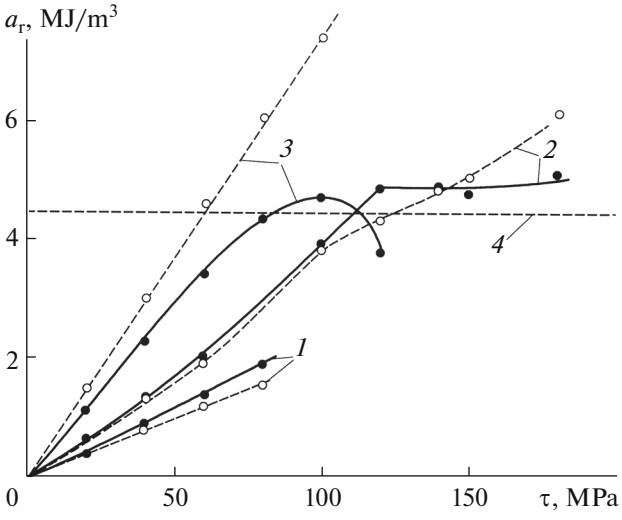


**Fig. 8.** Effect of counteraction stresses τ on the specific shape recovery energy $a_r$ of the alloy TN1 samples annealed at 570°C and deformed at 20°C by (*1*) 6, (*2*) 10, and (*3*) 20%. (solid lines *1*–*3*) Experimental results, (dashed lines *1*–*3*) calculation results, and (*4*) calculated maximum value of $a_r$.

The shape recovery energy at constant external counteraction can be calculated as the product of the counteraction stress into the strain recovered in heating. If the processes of slip and unrecovered strain accumulation are not taken into account, $a_r$ can be estimated by the expression

$$a_r = \frac{1}{2}\tau\left(\gamma_\tau - \frac{\tau}{G}\right),$$

where $\tau$ is the external counteraction stress (MPa), $\gamma_\tau$ is the strain accumulated by a sample during preliminary deformation by $\gamma_s$ and subsequent loading to $\tau$, and $G$ is the shear modulus (MPa; it is very low (~5.0 GPa) in the samples annealed at 570°C (see Table 1)).

Dashed lines *1–3* in Fig. 8 show the calculated dependences of $a_r$ on $\tau$ for various values of $\gamma_s$. It is clearly visible that, when slip is absent in the alloy (e.g., in the samples deformed by 6 and 10% at $\tau <$ 100 MPa), the calculated and experimental values of $a_r$ almost coincide. The difference between the calculated and experimental data is maximal for the samples deformed by 20%: slip in them hinders the reverse martensitic transformation upon heating.

The maximum values of $a_r$ in the samples annealed at 570°C were reached after deformation by 10% at normal temperature and the application of counteraction stresses of 120–180 MPa. We can conclude that the specific shape recovery energy is maximal in the material when its induced strain corresponds to $\gamma_{cr}^{0.3}$ and the shape recovery counteraction stresses are close to $\tau_{cr}^{0.3}$, all other thing being equal. It should be noted that these maximum strains and stresses, which result in full shape recovery after loading, unloading, and/or heating above $A_e^r$, are the limiting conditions under which a sample can be subjected to repeated cycling through the temperature range of the forward and reverse martensitic transformations and accumulate and recover strain without a substantial distortion of its initial shape.

The maximum possible level of the specific shape recovery energy under limited development of slip processes can be estimated by the formula

$$a_r^{max} = \frac{1}{2}\tau_{cr}^{0.3}\left(\gamma_{cr}^{0.3} - \frac{\tau_{cr}^{0.3}}{G}\right).$$

At $\gamma_{cr}^{0.3} = 9\%$ and $\tau_{cr}^{0.3} = 150$ MPa, the calculated maximum value of $a_r$ is 4.5 MJ/m$^3$, which is close to the experimental value (4.8–5.3 MJ/m$^3$).

The slightly lower values of calculated $a_r$ as compared to the experimental data are related to the fact that the shear modulus measured at 20°C was used in the calculations, whereas it is more correctly to use the shear modulus measured at 140–160°C. Upon heating, the shear modulus of the alloy should increase due to the transformation of martensite into austenite [15], and the specific shape recovery energy should also increase.

The structural state of the titanium nickelide–based alloy substantially affects the shape recovery energy (see Table 1). In the initial state (after drawing), high shape recovery energies after deformation at 20°C cannot be achieved because of the superelastic properties of the material and a very low residual strain. A theoretical analysis demonstrates that the maximum shape recovery energy of the material in this structural state does not exceed 1.0 MJ/m$^3$. Therefore, we did not determine the shape recovery energy of the samples in the initial state with a deformed structure. After polygonization annealing at 450°C, the samples have high critical stresses and a satisfactory critical strain. Therefore, we can reach a maximum specific shape recovery energy of 3.6 MJ/m$^3$. Recrystallization annealing at 570°C decreases the critical stresses; however, the critical strain increases under these conditions, which ensures a high maximum value of $a_r$ (~5.0 MJ/m$^3$).

An increase in the recrystallization annealing temperature to 900°C leads to *B*2-grain growth. This growth enhances the nonuniformity of the stress and microstrain distributions in the material volume and favors their concentration at grain boundaries [16]. As a result, slip in the material occurs at the macrostresses and macrostrains that are lower than those after annealing at $t = 450$ and 570°C, and their critical values decrease (see Table 1). The calculation of $a_r^{max}$ demonstrates that the maximum shape recovery energy is 3.4 MJ/m$^3$ at $\gamma_{cr} = 7.0\%$ and corresponding $\tau_{cr} = 120$ MPa, and this value agrees well with the experimental results (3.8 MJ/m$^3$).

## CONCLUSIONS

(1) Our investigations showed that the specific superelasticity and/or shape recovery energy is to be determined to describe the thermomechanical properties of an SME material and to calculate the operating characteristics of the articles made of it. For this purpose, the critical strains and stresses corresponding to the maximum loading of a sample, after which it completely (accurate to 0.2% for tension–compression and 0.3% for torsion) restores its shape after unloading and/or subsequent heating above $A_e^r$, should be determined from the results of loading at a temperature lower than $A_s^r$.

(2) The experiment to determine the maximum specific shape recovery energy $a_r^{max}$ should be performed under the conditions where the induced strain is $\gamma_{cr}^{0.3}$ and the counteraction stresses correspond to $\tau_{cr}^{0.3}$.

(3) The structural state of the samples of a titanium nickelide–based alloy was found to affect $\gamma_{cr}^{0.3}$, $\tau_{cr}^{0.3}$, and $a_r^{max}$. $\gamma_{cr}^{0.3}$ is maximal after recrystallization annealing. The critical stresses decrease and the critical strains increase when the lattice imperfection decreases during polygonization and recrystallization annealing. The specific shape recovery energy is maximal in samples with a recrystallized structure.

## ACKNOWLEDGMENTS

This work was performed in terms of the base part of state task 11.7449.2017/BCh for institutes of higher education using the equipment of the joint use center Aviation-Space Materials and Technologies at the Moscow Aviation Institute.

## REFERENCES

1. K. Ootsuka et al., *Shape Memory Alloys*, Ed. by Funakubo (Metallurgiya, Moscow, 1990).
2. *Shape Memory Alloys. Modeling and Engineering Applications*, Ed. by D. C. Lagoudas (Springer, 2008).
3. G. Song, N. Ma, and H.-N. Li, "Applications of shape memory alloys in civil structures," Eng. Struct., No. 28, 1266–1274 (2006).
4. T. W. Duerig and K. N. Melton, "Applications of shape memory in the USA," in *Proceedings of 1st Japan International Conference on New Materials and Processes for the Future* (Nippon Convention Center, Chiba, 1989), pp. 196–200.
5. M. Yu. Kollerov et al., *Functional Shape Memory Alloys: Tutorial* (INFRA-M, Moscow, 2016).
6. M. Yu. Kollerov et al., "Thermomechanical behavior of titanium nickelide actuators," Titan, No. 1 (55), 46–61 (2017).
7. D. B. Chernov, *Structural Application of Shape Memory Alloys*, Ed. By A. V. Mitin (Izd. NIISU, Moscow, 1999).
8. H. Sadiq et al., "The effects of heat treatment on the recovery stresses of shape memory alloys," Smart Mater. Str. **19** (3), 1–7 (2010).
9. A. Abdy, H. Sadiq, and R. al-Mahaidi, "Effect of heat treatment on the recovery stresses generated by superelastic NiTi shape memory alloy wires," in *Proceedings of 23rd Australian Conference on Mechanics of Structures and Materials (ACMSM23)* (Byron Bay, 2014), pp. 211–216.
10. D. E. Gusev, M. Yu. Kollerov, A. A. Sharonov, S. I. Gurtovoi, and A. V. Burnaev, "Reactive stresses in titanium nickelide-based alloys," Russ. Metall. (Metally), No. 5, 395–399 (2015).
11. *ASTM F2082/F2082M-16. Standard Test Method for Determination of Transformation Temperature of Nickel–Titanium Shape Memory Alloys by Bend and Free Recovery* (The American Society for Testing and Materials, 2016).
12. M. Yu. Kollerov et al., "Formation of the structure of a TN1 alloy during deformation and heat treatment," Titan, No. 3, 4–10 (2010).
13. A. A. Il'in et al., "Technological methods of control of the structure and thermomechanical properties of titanium nickelide–based alloys," Tekhn. Legk. Splav., No. 1–4, 18–23 (2005).
14. A. A. Il'in et al., "Mechanisms of shape changes upon deformation and heating of shape-memory titanium alloys," Metalloved. Term. Obrab. Met., No. 4, 12–16 (1998).
15. V. V. Khachin, V. G. Pushin, and V. V. Kondrat'ev, *Titanium Nickelide: Structure and Properties* (Nauka, Moscow, 1992).
16. A. A. Il'in et al., "Some innovative technologies in the production of medical implants made of titanium alloys," Tekhn. Legk. Splav., No. 3, 131–137 (2007).

*Translated by K. Shakhlevich*